# Distributed Speech Recognition within a Segment-Based Framework

by

Laura S. Miyakawa

B.S., Carnegie Mellon University, 2001

Submitted to
the Department of Electrical Engineering and Computer Science
in Partial Fulfillment of the Requirements for the Degree of

Master of Science

at the

Massachusetts Institute of Technology

June 2003



Signature of Author .....
Department of Electrical Engineering and Computer Science
May 21, 2003

Certified by .....
I. Lee Hetherington
Research Scientist
Department of Electrical Engineering and Computer Science

Accepted by .....
Arthur C. Smith
Chair, Department Committee on Graduate Students

# Distributed Speech Recognition within a Segment-Based Framework

by

Laura S. Miyakawa

Submitted to the Department of Electrical Engineering and Computer Science
in June, 2003 in partial fulfillment of the requirements for the Degree of
Master of Science

## Abstract

The widespread acceptance of personal digital assistants (PDAs) has led to research into the interaction people have with these devices. Speech is a natural choice for this interaction. However, traditional speech recognition systems require an abundance of memory and processor cycles. On limited machines like an iPAQ, implementing an entire speech recognition system would be debilitating to the device. A solution to this problem is to allow the iPAQ to communicate with a server that does the actual recognition task. This method is better known as distributed speech recognition (DSR).

This thesis examines the problems of implementing DSR on an iPAQ. We faced the challenge of reducing the bandwidth required by the system while maintaining reasonable recognition error rates. We examined using a fixed-point processing in reducing the computational demand put on the iPAQ. The word error rates for the baseline floating-point front-end system and our fixed-point front-end were 9.8% and 9.6% respectively. However, using the fixed-point front-end actually increased our bit rate. Next, we focused on the effects of quantizing Mel-Frequency Cepstral Coefficients (MFCCs) before sending them to a recognizer on the server side. We evaluated both scalar and vector quantizers using non-uniform bit allocation. Our optimal vector quantizer reached a word error rate of 9.8% at 6400 bps. Finally, because our recognizer further processes the MFCCs to arrive at boundary measurements, we explored the idea of quantizing these boundary measurements. The scalar boundary measurement quantizer reached a word error rate of 9.6% at 150 bits per hypothesized boundary. We averaged 21.1 hypothesize boundaries per second on our test data; thus, we could transmit boundary measurements at 3165 bps and maintain a 9.6% word error rate.

**Thesis Supervisor:** I. Lee Hetherington
**Title:** Research Scientist

# Acknowledgments

I would like to acknowledge my thesis advisor Lee Hetherington for his patience, flexibility and willingness to help me debug code. I also need to thank Scott Cyphers for his help with the iPAQ and the audio server. A debt of thanks is owed to the Spoken Language Systems group in its entirety for all the critical thinking they put into this thesis. Naturally, included in that is my office. Han, Ernie and Alicia have a special place for all of help they have given me. From basic concept understanding, to writing scripts, to just putting up with all my chatter, these three have seen it all.

Outside of research, I need to thank the 6.1 girls for all their support and advice in navigating MIT. As well, my family for lending me support from afar and always keeping things interesting at home. And finally, I have to thank Jeff for doing the dishes and the laundry when I've been slaving away at the office, for helping me design some of the figures in this thesis, and for basically being wonderful.

This research was supported by a Lucent fellowship and by DARPA under Contract N66001-99-1-8904 monitored through the Naval Command, Control, and Ocean Surveillance Center.

# Contents

# List of Figures

# List of Tables

# Chapter 1

# Introduction

## 1.1 Problem Definition

The widespread acceptance of personal digital assistants (PDAs) has led to research into the interaction people have with these devices. Because they are too small to have traditional keyboards, developers are constantly looking at better ways to manipulate these hand-helds. Speech is a natural choice for this interaction. Speech requires no special learning on the part of the user and enables the screen of the PDA to be used for other things. However, traditional speech recognition systems require an abundance of memory and processor cycles. On limited machines like an iPAQ, putting an entire speech recognition system on it would be debilitating to the device. A solution to this problem is to allow the iPAQ to communicate with a server that does the actual recognition task. This method is better known as distributed speech recognition.

There are two main problems faced when implementing a distributed speech recognizer. The first is how to choose which parts of the recognition process are handled by the server and which by the client (the iPAQ in our case). Many systems have been built that employ server-only processing. When this is the scheme used, the speech is merely compressed on the client side then transmitted to the server for expansion, feature extraction, and recognition. Another common place to break up the computation flow is at the feature level. Here, the features are computed by the client, then quantized and sent to the server for recognition. This scheme has the added advantage that feature vectors tend to be more robust to quantization than the original signal and, therefore, require less bandwidth than original waveform. The second problem faced by distributed speech recognition stems from the necessity to quantize. In many packet-based transmission schemes or narrow-band channels the bit rates of these features are unattainable. Thus, we are forced to quantize these

features to a feasible bit rate. If the quantization scheme is chosen carefully, it can actually improve the accuracy of the recognizer by removing unnecessary information.

## 1.2 Previous Work

For this thesis we looked at work done both in the implementation of fixed-point processing and in distributed speech recognition.

### 1.2.1 Fixed-Point Front-End

In an attempt to lower power consumption on the Hewlett Packard Labs Smartbadge IV that is the client of a distributed speech recognition system, Hewlett Packard implemented a fixed-point front-end [3]. The Smartbadge IV uses a fixed-point strongARM processor which has a floating-point emulation program to run floating-point code similar to the processor used in the iPAQ. Hewlett Packard used the HMM-based SPHINX II recognizer as their baseline system. They did not concern themselves with the compression and transmission of their features, merely the computation of them. The real-time factor for each code version of their front-end can be seen in Figure 1.1. The real-time factor is the amount of time to process 1 second of speech. Here, for example, the baseline system takes 1.51 seconds to process 1 second of speech. The optimized floating-point code included special FFT algorithms which reduced the size of the FFT by half. They also implemented an optimized floating-point front-end that used 32-bit floating-point calculations. The fixed-point system reduces the computation time of the baseline by 98%. The word error rate (WER) for all of the systems except the fixed-point version is 4.2%. For the fixed-point system the word error rate is 4.3%. This increase of 0.1% was eliminated by training on fixed-point front-end data.

### 1.2.2 Distributed Speech Recognition

In the interest of performing speech recognition over the Internet or over cellular telephones much work has been done in the quantization of features. Some of this work focuses on the quantization of Mel-Frequency Cepstral Coefficients (MFCCs) [4]. Others focus on the quantization of coded speech for both recognition and synthesis [9, 11].

One study that focused on speech recognition over the Internet looked at speech compression algorithms and scalar and vector quantization of MFCCs [4]. Their first experiments were doing server-only processing. They used both $\mu$-Law and GSM compression algorithms, but neither proved to be a reasonable method since both

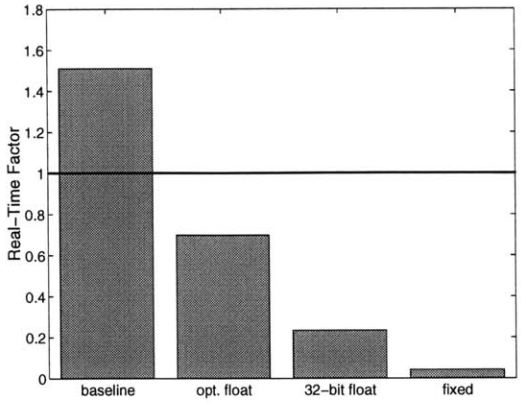


Figure 1.1: Real-time factors for each version of front-end code from [3].

| | Bit Rate (Kbps) | WER |
|---|---|---|
| Baseline | – | 6.55% |
| constant bits per coefficient, non-uniform | 10.4 | 6.53% |
| | 3.9 | 6.88% |
| variable bits per coefficient, non-uniform | 3.0 | 6.55% |
| | 2.4 | 6.99% |
| Vector Quantization | 2.0 | 6.63% |

Table 1.1: Some results from Digalakis, et al, 1999 [4].

doubled the baseline word-error rate. They also explored using both uniform and non-uniform scalar quantization of the MFCCs with a constant number of bits per coefficient. Some of their results are reported in Table 1.1. Here, they found they could reduce the bit rate to 3.9 Kbps and only increase the WER by 5% relative when using non-uniform scalar quantization as seen in Row 3 of Table 1.1. In addition they explored scalar quantization where the number of bits per coefficient could vary. Doing this allowed them to decrease the bit rate to 2.8 Kbps and slightly improve the word error rate over the constant bit allocation method. Finally, they tried product-code vector quantization (VQ). To determine subvectors they used both correlation-based partitioning and knowledge-based partitioning. Knowledge-based partitioning outperformed the correlation-based partitioning. This may have been caused by the small data set used to determine the correlation-based partitioning or the low correlation between coefficients leading to arbitrary partitioning. The results of one test using knowledge-based partitioning is shown in Table 1.1.

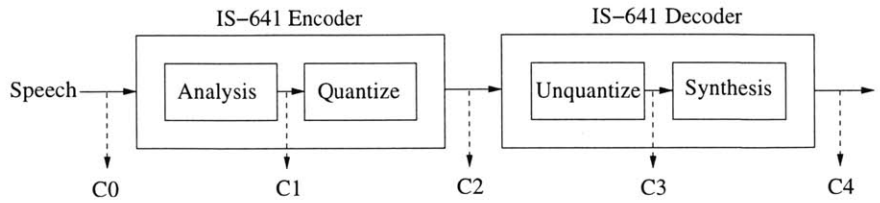

Figure 1.2: Diagram of of IS-641 Encoder and Decoder with locations where features are extracted labeled with C$x$ from [11].

In another study perceptual linear predictive analysis (PLP) was quantized and transmitted for distributed recognition [9]. PLP is similar to LPC (linear predictive coding) in that it creates and all-pole model for each frame of the speech. It differs because it exploits some auditory perception information to reduce the number of parameters needed per frame. They quantized and unquantized these parameters using vector quantization and used dynamic time warping to recognize the digit sequence. They showed the remarkable ability to reduce the bit rate to 400 bps with statistically similar word error rates to using no quantization. At this rate both PLP and speech coder parameters could be transmitted over a standard cellular channel.

A fairly comprehensive study used the IS-641 coder and explored using features from different parts of the coding stream for recognition [11]. The IS-641 coder can be thought of in two blocks, an analysis block which is similar to LPC analysis and a quantization block. They look at the word error rates generated when features are computed from the original speech waveform, from just after the analysis block, from just after the unquantization, and from the decoded speech as shown in Figure 1.2 by the labels C0 through C4. They also did experiments training on one set of features and testing on another. In addition they ran tests on large vocabularies, recognition in the presence of noise, and recognition with channel impairments. They found that when they included voicing information with features generated at C3, they got statistically similar results to those using features derived from the original speech, C0.

## 1.3 Goals and Overview

This project was motivated by the desire to reduce the bandwidth needed in a distributed speech recognition system on an iPAQ. Earlier work by Scott Cyphers of SLS yielded a recognition system that included an iPAQ client that transmitted an $\mu$-law utterance to a server for recognition. To reduce the bandwidth required, we needed to do more than just compress the speech waveform. Previous work by Jon Yi of SLS showed that by quantizing the MFCCs with a uniform scalar quantizer,

the bandwidth needed to transmit MFCCs could be decreased while the recognition accuracy remained unchanged.

This thesis can, then, be viewed as three distinct parts. The first is the creation of a fixed-point front-end for execution on the iPAQ. The second is the study of the the effects of quantization of the cepstral coefficients on the word error rate of the recognizer. The third is the investigation of the effects of quantization of the boundary measurements on the word error rate of the SUMMIT recognizer.

Because the iPAQ uses a fixed-point StrongARM processor, we implemented a fixed-point front-end to compute the cepstral coefficients. The goal of this portion of the project was to translate our floating-point front-end into fixed-point computation avoiding the pitfalls of overflow while reducing the computations needed on the iPAQ.

Once the cepstral coefficients were computed, we performed non-uniform scalar and vector quantization and looked at the effects on word error rate. We used a greedy algorithm to do bit allocation where a variable number of bits are used for each of the cepstral coefficients. In addition we computed the covariance matrix for the MFCCs and used several algorithms to come up with good covariance-based partitions for product-code VQ. We also tried knowledge-based partition methods for product-code VQ similar to [4].

Many people have studied putting the computation of MFCCs on the client. This is natural for a recognizer that is HMM-based since its features are MFCCs. In our SUMMIT recognizer, however, we perform additional computations to compute boundary measurements for our features. Because of this difference we explored the effects of quantizing these boundary measurements with both scalar and vector quantization methods. Scalar and vector quantization tests similar to the ones done on the MFCCs were run on the boundary measurements with a few differences. Because the boundary measurements are derived to be uncorrelated with each other, covariance-based partitions were not explored. We did explore weighting the bit allocation by the eigenvalues.

Chapter 2 goes into the background for front-end processing, scalar and vector quantization and fixed-point processing. Chapter 3 discusses the research issues encountered when implementing the fixed-point front-end. In Chapter 4, we give results for the experiments in quantizing the MFCCs. Chapter 5 reports the results from recognition experiments using quantized boundary measurements. Finally Chapter 6 summarizes and draws conclusions.

# Chapter 2

# Background

In this thesis we deal with the ideas of creating a fixed-point front-end and quantizing feature vectors. In the following sections we give background information on how the MFCCs are computed in the front-end, boundary measurements computation, fixed-point numbers, and quantization.

## 2.1 Mel-Frequency Cepstral Coefficients

Mel-Frequency Cepstral Coefficients (MFCCs) are a commonly used representation of the speech waveform. They are the features used most regularly in HMM-based speech recognizers and are intermediary features within the MIT SUMMIT segment-based recognizer. Some good references for the computation of MFCCs are [5, 17]. A block diagram of the front-end which computes the MFCCs is included in Figure 2.1. A brief description of each block is given.

Speech starts as a continuous waveform. It is recorded and discretized. In order to process it, we break it into small overlapping blocks or frames and analyze each frame's frequency content. This first dividing of the stream of speech into individual frames occurs in the *Framing* block. In our system we compute a frame every 5 ms, and each frame is 25.6 ms long. We will use $x_i[n]$ to represent the $i^{th}$ frame of the input speech.

Next, we run each block through a pre-emphasis filter $p[n]$ (as defined in Equa-

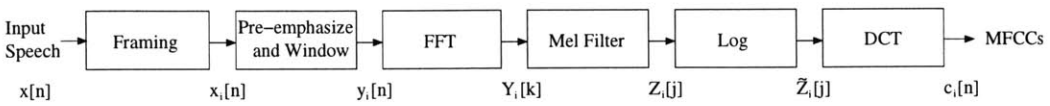


Figure 2.1: Illustration of the front-end.

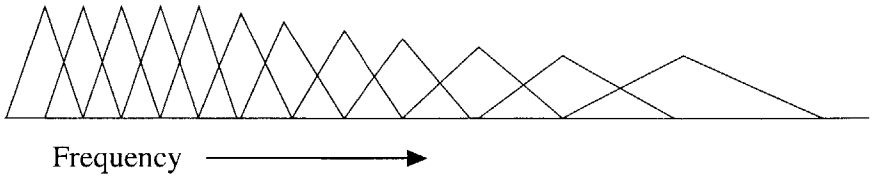

Figure 2.2: Illustration of the Mel-Scale Filter Bank.

tion 2.1) which puts more emphasis on the high-frequency regions of the waveform. We apply this gentle high-pass filter to counteract the radiation characteristics of the mouth. We, then, multiply the block by a window $w[n]$. Here, we use a Hamming window which tapers toward its edges to minimize the interference effects from framing. Let $y_i[n]$ represent the output of the *Pre-emphasize and Window* block.

$$p[n] = \delta[n] - .97\delta[n-1] \tag{2.1}$$

$$y_i[n] = w[n](p[n] * x_i[n])$$

Next we take an FFT. The FFT computes the frequency spectrum of the frame. $Y_i[k]$ is the output of the FFT and is given by:

$$Y_i[k] = FFT\{y_i[n]\}$$

Now that we have the frequency spectral information we can filter it into various bands. Illustrated in Figure 2.2 is an approximation of the Mel-Scale Filter Bank we used[2]. A Mel-Scale Filter Bank has filters which are linearly spaced in the low frequency range and logarithmically spaced in the high frequency range. This means that in the high frequency range we are melding more of the frequencies together than in the low frequency range. This filter bank approximates how the human ear filters the frequencies it encounters. We apply this filter bank to the square of the magnitude of $Y_i[k]$ The output of the filters is $Z_i[j]$, and the Mel-Filter bank is $H_j[k]$.

$$Z_i[j] = \sum_{k=0}^{N/2} |Y_i[k]|^2 H_j[k] \tag{2.2}$$

The next block is the *Log*. This block takes the natural log of the output of the Mel Filters.

$$\tilde{Z}_i[j] = \ln(Z_i[j])$$

The *DCT* block is a Discrete Cosine Transform. In this scenario it yields the same results as an IFFT (taking frequency information and transforming it into the time

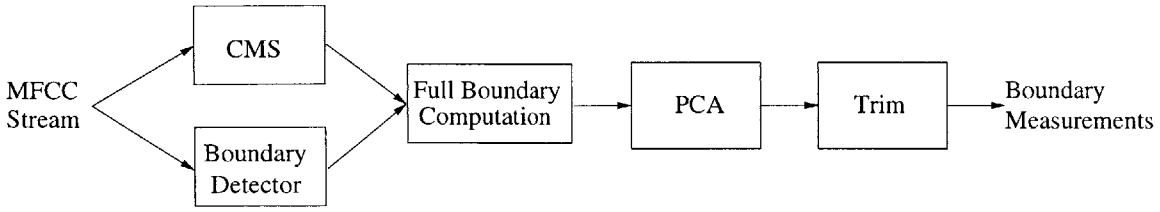


Figure 2.3: Illustration of the computation of boundary measurements.

domain), but uses less computation. Because we have an FFT, Log and DCT in sequence, we are transforming our data into the cepstral domain, creating MFCCs. We save only the first 14 MFCCs, $c_i[n]$.

$$c_i[n] = DCT\{\tilde{Z}_i[j]\}$$

We compute the cepstrum to deconvolve the source from the filter [13, 14, 19]. In our case the vocal source is either vibration from the vocal folds or noise, and the filter is derived from the shape of the vocal tract. It is the shape of the vocal tract that gives speech the spectral characteristics we distinguish to understand different sounds. Getting rid of the vocal source is desired in speaker-independent speech recognition systems since, in English, pitch information does not give us information about the words that were spoken. In fact we hope to throw away pitch information so the same models can be used for speakers with different speaking pitches.

## 2.2 Boundary Measurements

A typical speech recognizer uses an HMM with MFCCs as its features. The SUMMIT system, however, goes a few steps further in processing to get features which represent boundary measurements [8]. A block diagram of how we get from MFCCs to boundary measurements is in Figure 2.3.

The MFCC stream computed in the previous section is used in two different blocks. One is Cepstral Mean Subtraction (CMS) [10, 17, 7]. Mathematically, this is just computing the mean for each coefficient across all the frames in the utterance and subtracting that mean from each cepstral vector as seen in Equation 2.3. Since we are dealing with the cepstrum, responses that were convolved in the time domain are now added. By subtracting off the mean, we are essentially subtracting off any constant convolutional effects. One example of a constant convolutional effect is the frequency response of the room. By subtracting off the mean, speech that is recorded in an opera house and speech recorded in a closet should yield the same features.

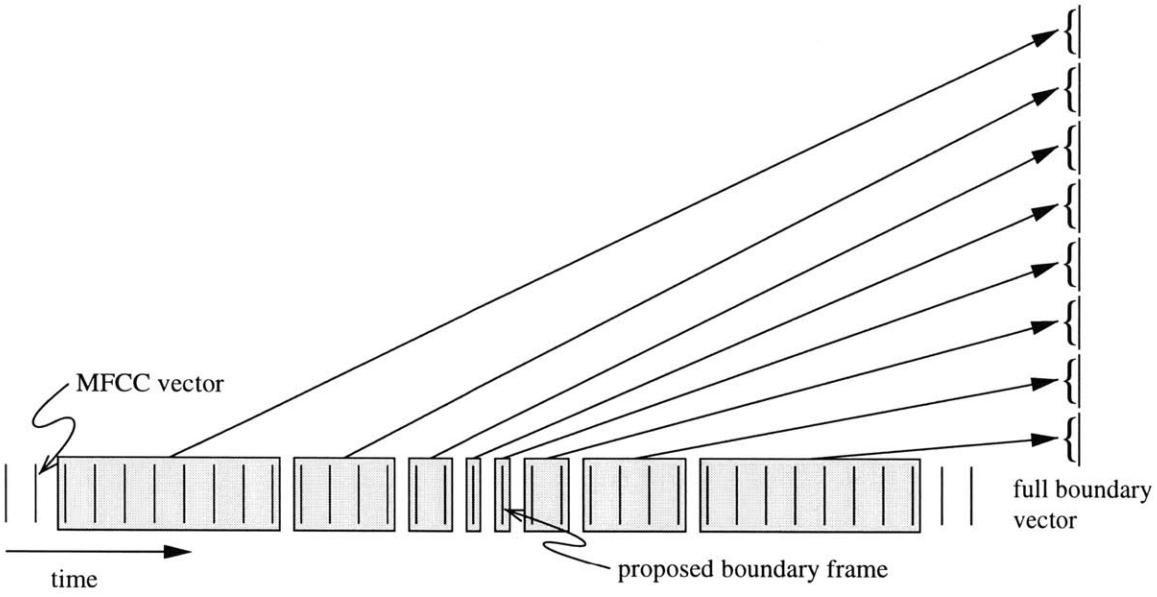


Figure 2.4: Illustration of full boundary measurements computation.

$$\bar{c}_i[n] = c_i[n] - \frac{1}{T}\sum_{j=1}^{T} c_j[n] \tag{2.3}$$

The simultaneous block *Boundary Detector* hypothesizes where boundaries between segments may be. A segment can be thought of as one phone, so in the word `bad` boundaries should be detected between the `b` and the `a` and between the `a` and the `d`.

Once frame $j$ is hypothesized as a boundary frame, the frames around it are buffered and averaged together in the *Full Boundary Computation* block. A schematic of what goes on in this block is included in Figure 2.4. In this figure the vertical hashes represent a vector of normalized MFCCs. The shaded boxes in Figure 2.4 show which vectors get averaged together. For example, if the proposed boundary frame is $\bar{c}_j[n]$, then $\bar{c}_{j+1}[n]$ and $\bar{c}_{j+2}[n]$ will be averaged together as will $\bar{c}_{j-4}[n]$, $\bar{c}_{j-5}[n]$, $\bar{c}_{j-6}[n]$ and $\bar{c}_{j-7}[n]$. This yields 8 averaged cepstral vectors, each of length 14, which are then stacked to create one very big full boundary vector of length 112.

The next block, *PCA*, does a principle component analysis that multiplies the boundary vector by a rotation matrix which approximately makes the coefficients uncorrelated. The output vector is still of length 112, but now the coefficients are ordered by variance with the coefficients with highest variance first. We then trim this

vector down (in the *Trim* block) to its first 50 coefficients to reduce the computational demand. This paring down of the boundary vector also aids in classification because higher dimensional features require more training data. Because of the ordering imposed by the *PCA*, we know that we are keeping the 50 coefficients that have the highest variance and hopefully the 50 most important coefficients.

## 2.3 Fixed-Point Numbers

A fixed-point number is an integer that the programmer can interpret as rational number. When you use a floating-point number to represent fractional information, you have no control over how many bits and, therefore, how much accuracy, is assigned to that fraction. Your computer handles this and increases or decreases the number of bits used for the fractional portion of a number depending on the resolution needed. In a fixed-point number the developer gets to decide how much resolution is given to the fractional information. The best way to explain this is in an example. Let's assume that we have an unsigned 8-bit fixed-point number. To keep track of the number of bits used for the fractional information (or behind the decimal point), we adopt a $Qn$ notation where $n$ designates the number of fractional bits [3]. Let say the binary representation of our number is `01101011`. If this number is in $Q0$ then there are 0 bits behind the decimal point, and, thus, all bits are used for the integer portion of the number, so we would interpret it as the number 107.

$$\texttt{01101011.} = 2^6 + 2^5 + 2^3 + 2^1 + 2^0 = 107$$

If this number is in $Q1$, then the last bit is used for the fractional portion. Similar to how each bit represents a positive power of two in binary, any bits used behind the decimal points now pertain to the negative powers of two.

$$\texttt{0110101.1} = 2^5 + 2^4 + 2^2 + 2^0 + 2^{-1} = 53.5$$

If this number was in $Q6$ format, it would represent:

$$\texttt{01.101011} = 2^0 + 2^{-1} + 2^{-3} + 2^{-5} + 2^{-6} = 1.671875$$

There are a few things to note. First 53.5 is half of 107. 1.671875 is 1/64 of 107. In fact, to translate any integer into its $Qn$ value, simply divide that integer by $2^n$. Another point to consider is the trade-off between the largest integer that can be represented and the resolution of the fractional portion. Notice that in $Q6$ the largest integer that can be represented is 3 while in $Q0$ it is 255. This factor comes into play when one must consider the possibility of overflow in computation. We will explore this problem further in Chapter 3.

## 2.4 Quantization

Quantization is the process of considering a variable that could take on any value (continuous-amplitude) and restricting it to take on only a discrete set of values [20]. In this way a value can be represented with less information (bits). Most quantization schemes follow the method below.

- *Initialize:* Choose a number of levels or bins. Determine which ranges of values belong to each bin. Choose a representative (or quantized) value for each bin. Assign each bin a label.

- *Quantize:* For a given value of a variable, choose the bin it falls into and record its bin label.

- *Unquantize:* Translate each bin label to the representative value of that bin.

A key metric of how well a quantizer works is a distortion measure (also known as a dissimilarity measure or a distance measure). The distortion measure gives information about the difference between the original value and the quantized value.

A simple quantization example is a street address on a letter; it has many levels of quantization. Let's let our distortion measure be the likelihood that a letter delivered to the quantized address will get to me. The letter will start with just my name on it and a 37 cent stamp. First let's think about how the state in the address is an example of quantization. There are 50 states, so there are 50 quantization levels. the range of each bin is determined by the state boundaries. Let the quantized value for each state be the address of city hall in the state's capital. The label for each bin is the state's two letter abbreviation. On the state level my address is quantized to the label **MA** and is unquantized to the address of the state house. Since it is unlikely that any mail delivered to Beacon Hill would make it to my house in Somerville, we can say the quantization error is high. Next we quantize each state. Each state is quantized by city. Let the quantized value of the address now be city hall. My address is now quantized to the label **Somerville, MA** and unquantized to the address of city hall in Somerville. At this level of quantization, it is slightly more likely that I will get the piece of mail, but the odds are still against me. At this point, let's consider the zip code. A zip code contains information about not only state and city, but also about a zone within a city. If we let the quantized address be the address of my local post office, then my chances of getting the letter might be estimated at about 50/50. And the process continues. The post office uses these course to fine quantizers to ensure that a letter can be easily deliverable with a reasonable amount of information in the address.

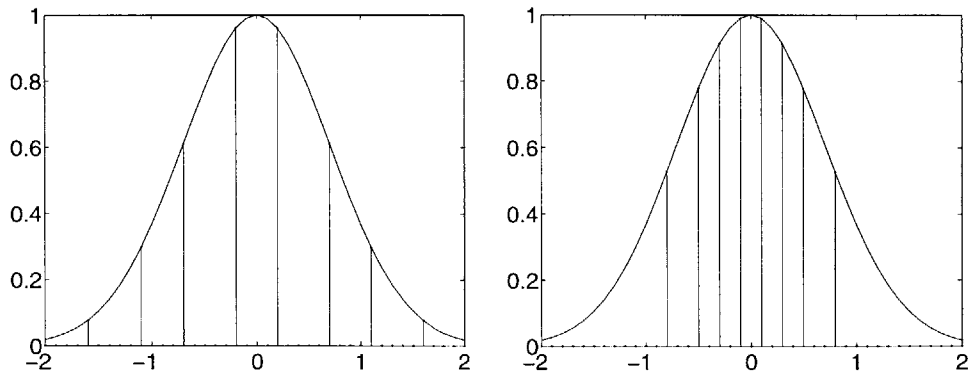


Figure 2.5: Illustration of Uniform Quantization Scheme in 2.5(a). Illustration of Non-Uniform Quantization Scheme in 2.5(b).

### 2.4.1 Scalar Quantization

Scalar quantization is just the quantization of each variable by itself. There are two main schemes of scalar quantization: uniform and non-uniform. In uniform quantization, sometimes called linear quantization, the bins are equally spaced across all possible values. Non-uniform quantization merely implies that the bins are not of equal size. A common non-uniform schemes uses information about the probability distribution of a variable to make each bin have the same probability of occurring. Examples of each are shown in Figure 2.5. In these figures the vertical lines represent the boundaries of the bins, and the curve is a Gaussian distribution for the variable being quantized. In the uniform quantization example, each bin has the same width. In the non-uniform quantization scheme, the bins are narrower where there is a higher probability of a value occurring. The advantage of the non-uniform scalar quantization is that by having bins of variable size, the expected value of the distortion measure can be minimized [12]. In reality we tend not to know the underlying statistics of our variables. To handle this problem we train our quantizers on the type of data it will see to approximate the distribution of the variable.

The most common distortion measure is the mean-square error (mse) [12]. Here we represent the $i^{th}$ value of our original variable $x$ as $x_i$, its quantized value as $\tilde{x}_i$,

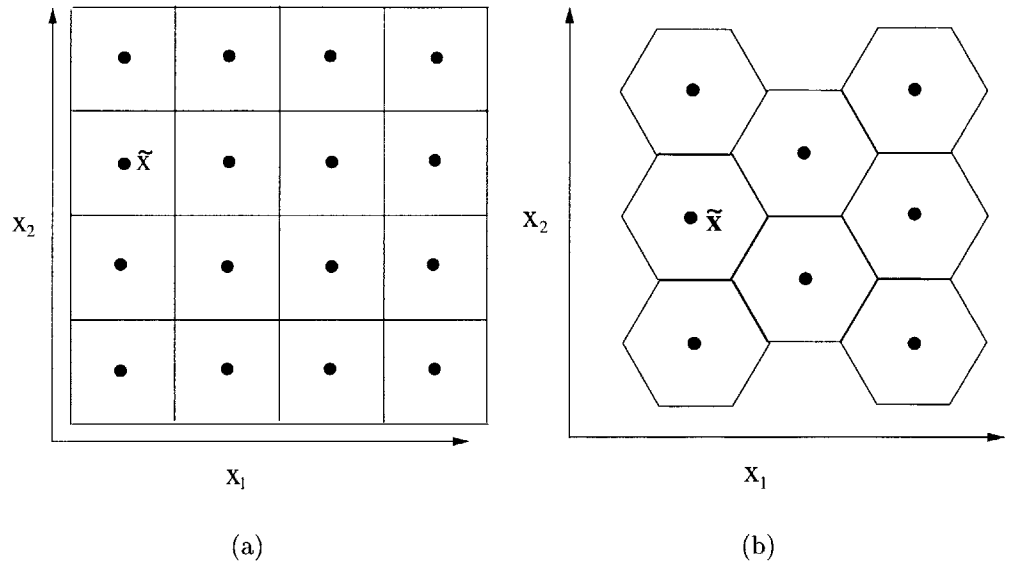


Figure 2.6: Illustration of a Uniform Scalar Quantization Scheme for a 2-D vector shown in 2.6(a). Illustration of a Uniform Vector Quantization Scheme for a 2-D vector shown in 2.6(b).

and the mean-square error as $d(x, \tilde{x})$.

$$d(x, \tilde{x}) = \frac{1}{N} \sum_{i=1}^{N} (x_i - \tilde{x}_i)^2$$

### 2.4.2 Vector Quantization

Instead of quantizing just one continuous variable, let's consider the quantization of a vector of continuous variables [18]. Let $\mathbf{x} = [x_1 x_2 \ldots x_N]^T$. For visualization purposes we will deal with the 2 dimensional case. Figure 2.6 shows two uniform vector quantization schemes. Both of these quantizers partition the space into a uniformly shaped bin and then choose a quantization value for that bin. As we get into higher dimensional spaces it is harder to choose a shape for a bin. Especially when we know little about the statistics of this data. In this case we train our quantizer on a randomly selected set of real data points. In the *Initialize* stage now, we use a clustering algorithm to divide our training data into appropriate bins. We then choose a point within each bin to be the quantization value, commonly the average of the points in a given bin. In the *Quantize* step, then, in order to find the bin that a

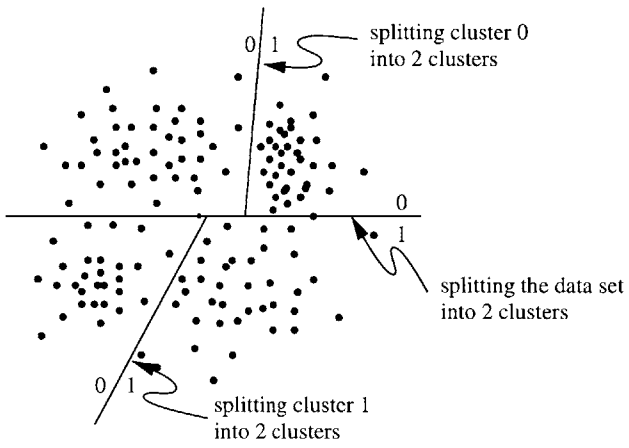

Figure 2.7: Illustration of binary splitting training.

new vector falls into we need only compute the distortion measure between the vector and the quantized value: the quantized value with the lowest distortion measure gives us the bin to which the vector belongs.

Two important metrics for any quantizer are the number of computations and the amount of storage it requires [12]. Let $N$ be the dimensionality of the random vector - in the case of a mse distortion measurement $N$ is also the number of multiply-adds needed per distortion computation. In a standard vector quantizer we expect the computational cost $C$ to be $C = NL$ where $L$ is the number of levels in the vector quantizer. In addition the storage cost $M$ is given by $M = NL$. Computing the distortion measure for every quantized value can be expensive. One way that we avoid this is to use binary splitting. Instead of clustering the training data right away into the desired number of bins in the *Initialize* step, first we cluster it into 2 clusters and we record the average vectors for each cluster. We then cluster each of those clusters into 2 clusters, recording their average vectors and so on, until the desired number of quantization levels is reached. Then when the test data is quantized, it is compared to the first pair of average vectors, the cluster to which it belongs is determined, and a 0 or 1 is recorded specifying its cluster. Then it is compared to the next pair of average vectors, and so on until it is in a single bin. This has the added advantage that by recording a 0 or 1 at each decision, we are writing down the bin label. This is illustrated in Figure 2.7. If a binary splitting vector quantizer is implemented the computation cost drop significantly to $C = 2N \log_2 L$. However, the storage costs now increase because we are left storing intermediate vectors at each stage of the binary splitting. The storage cost for binary splitting is given by $M = 2N(L-2)$. One way to reduce the amount of storage necessary is to do product code quantization where one splits the vector into subvectors and quantizes

each independently. For example, if we were to split our vector into two subvectors of dimensionality $N_1$ and $N_2$ and quantize them to levels $L_1$ and $L_2$, respectively, then the overall storage for a standard vector quantizer would be $M = N_1 L_1 + N_2 L_2$. Product code quantization does not necessarily reduce the computational costs. One condition in which the computational costs may be reduced is when the component vectors are quantized independently and the distortion measure is separable. If this is the case then the computational costs are reduced similarly to the storage costs. With product code vector quantizers, as with all quantizers, an optimal quantizer will minimize distortion. An optimal product code quantizer occurs if all the subvectors are statistically independent. If subvectors are not independent, that dependency will effect the quantizer's performance. To maximize performance of a product code vector quantizer, the number of subvectors should be small and the number of quantization levels should be big.

## 2.5 Chapter Summary

In this chapter we have reviewed the necessary knowledge for understanding the research that follows. Comprehension of the production of MFCCs and fixed-point numbers is necessary for creating a fixed-point front-end. The sections on quantization and MFCC computation cover material that is seen again in Chapter 4. Finally, knowledge of both quantization and the creation of boundary measurements will be used in Chapter 5. This chapter is not conclusive. Please review the references for further discussion on the topics presented here.

# Chapter 3

# Fixed-Point Front-End

In this chapter we delve into the specifics of creating a fixed-point front-end for the creation of MFCCs on the iPAQ. First, we cover the main differences in the algorithms for fixed-point versus floating-point front-ends. Next, we talk about the testing configuration under which our experiments were performed. Finally, we will discuss the resulting word error rates using the fixed-point front-end and some directions further research in this area could take.

## 3.1 Algorithm Optimization

In some parts of the computation of MFCCs, the algorithms remain very much the same in the fixed-point front-end as in the floating-point front-end, but others have had to be re-engineered to yield similar results. In this section we revisit the front-end computation flow, as previously shown in Figure 2.1, highlighting the major differences in the algorithms.

### 3.1.1 Framing, Pre-emphasis, Window

The framing block is not included in the fixed-point front-end; it is handled by the audio server in our implementation. The fixed-point front-end starts by being handed $x_i[n]$, an array of 16-bit integers from the audio server. We immediately translate $x_i[n]$ into $Q8$ by shifting each element 8 bits to the left. We know that this will not cause overflow because the numbers were shorts to begin with, and we are using 32-bit arithmetic. In the pre-emphasis step we store the factor 0.97 as a $Q8$ fixed-point number as well. When two fixed-point numbers are multiplied together their $Qn$ factors add. So, by applying this factor to an element of the array, we end up with a number in $Q16$ which we promptly shift back to $Q8$. Again here, there is no risk of

overflow.

The windowing step is where we first start making changes to accommodate for the fixed-point processing. The window we use is a Hamming window which can be derived by the equation below.

$$w[n] = \begin{cases} 0.54 - 0.46\cos(2\pi n/M) & 0 \leq n \leq M \\ 0 & \text{otherwise} \end{cases}$$

All the values in the Hamming window are, therefore, less than one, so we choose to represent them in $Q8$. Because we do not have a fixed-point cosine function, we must compute them using floating-point computations and translate them to fixed-point. To avoid computing this window for every frame, we compute the window just once upon instantiation and store it for use with every frame thus reducing our floating-point and translation computations. There is low risk of overflow when applying this filter.

### 3.1.2 FFT and the Mel Filter Bank

Because FFTs have become a very common computation in many fields, they have been implemented in both fixed-point and floating-point, in hardware and in software. The fixed-point FFT we use is derived from one developed by HP based on "Numerical Recipes in C" [3, 16].

When we square the output of the magnitude of the FFT, we are in real danger of overflow. Upon further inspection of Equation 2.2 (reproduced below),

$$Z_i[j] = \sum_{k=0}^{N/2} |Y_i[k]|^2 H_j[k]$$

we can rewrite it as:

$$Z_i[j] = \sum_{k=0}^{N/2} \left( |Y_i[k]| \sqrt{|H_j[k]|} \right)^2 \tag{3.1}$$

From Equation 3.1 we can delay the square until after the Mel Filters have been applied. This is advantageous because the amplitudes of the Mel Filters are less than one; thus, their square roots are also less than one. By multiplying by the Mel Filters before the square, we greatly reduce the risk of overflow. Similar to the Hamming window, the components of the Mel Filters are computed upon instantiation using floating-point code, translated to fixed-point and cached; thus, storing their square roots does not increase our storage cost and has no effect on the post-initialization computation cost.

However, by using Equation 3.1, we must now compute $|Y_i[k]|$. In floating-point front-ends $|Y_i[k]|^2$ is computed directly from the real and imaginary parts of $Y_i[k]$ without computing $|Y_i[k]|$. Doing a fixed-point square-root is very difficult, so we use an approximation suggested in [3, 6].

$$|x| \approx \alpha \max(|\Re\{x\}|, |\Im\{x\}|) + \beta \min(|\Re\{x\}|, |\Im\{x\}|) \tag{3.2}$$

To estimate $\alpha$ and $\beta$ we use polar coordinates and minimize the distance between $r$ and the estimate for $|x|$. For the following derivation we assume that the real part is bigger than the imaginary part. This narrows the range of $\theta$ to 0 to $\frac{\pi}{4}$. If the opposite were true, swapping $\alpha$ and $\beta$ would result in the correct approximation.

$$\Re\{x\} = r\cos\theta \quad \Im\{x\} = r\sin\theta$$

$$\min_{\alpha,\beta}(r - (\alpha r\cos\theta + \beta r\sin\theta))^2$$

$$\frac{\partial}{\partial\alpha} = 2(-r\cos\theta)(r - \alpha r\cos\theta - \beta r\sin\theta) = 0$$

$$\frac{\partial}{\partial\beta} = 2(-r\sin\theta)(r - \alpha r\cos\theta - \beta r\sin\theta) = 0$$

$$\int_0^{\pi/4} \frac{\partial}{\partial\alpha} d\theta = -sin\theta + \alpha\left(\frac{1}{2}\theta + \frac{1}{4}\sin 2\theta\right) - \frac{\beta}{2}\cos^2\theta\Big]_0^{\pi/4} = 0$$

$$\int_0^{\pi/4} \frac{\partial}{\partial\beta} d\theta = \cos\theta - \frac{\alpha}{2}cos^2\theta + \beta\left(\frac{1}{2}\theta - \frac{1}{4}\sin 2\theta\right)\Big]_0^{\pi/4} = 0$$

$$\alpha = 0.9475 \quad \beta = 0.3925$$

The error for this approximation is given in Figure 3.1. In this figure the actual magnitude has been held at 1, while the angle $\theta$ was swung through 0 to $\frac{\pi}{4}$. The maximum error, achieved at $\theta = 0$ or $\theta = \frac{\pi}{4}$, is .0525. The average value of the error is on the order of $10^{-4}$.

Thus, to compute the outputs of the Mel filter bank without overflow, we approximate the magnitude with Equation 3.2, multiply the magnitude by the root of the Mel filter parameters and square the outputs of the filters.

### 3.1.3 Natural Log and DCT

The computation of the natural log is another place where a new algorithm must be derived to handle fixed-point numbers. Because the representation of numbers in a computer is inherently binary, we choose to implement a fixed-point log base-2 and then scale by ln(2) to arrive at the natural log. This base-2 log algorithm was used in [3] and developed by [1]. The algorithm follows.

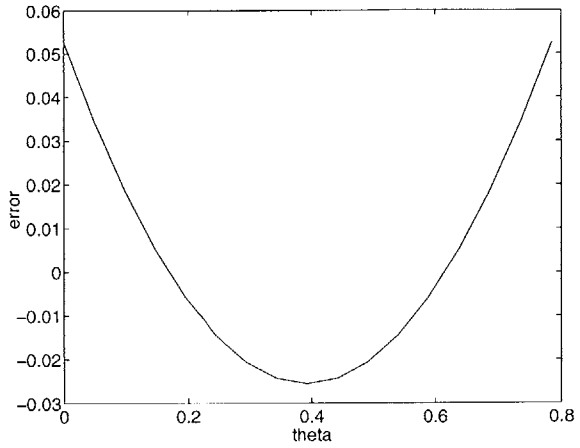


Figure 3.1: Plot of error versus angle for magnitude approximation when actual magnitude is held constant at 1.

- Find the position of the leftmost 1 when the number is represented in binary. The lowest order bit is position 0. Let that position be $b$
- Interpret the three bits to the right of position $b$ on their own. Call this number $n$.
- The approximation for the log is $8b + n$ in $Q3$

Here is an example using the number 50. The log base-2 of 50 is 5.644. We represent 50 in binary as `00110010`. $b$ for 50 is 5 since the leftmost 1 is in position 5. The next three bits after position 5 are `100` thus $n = 4$. Our estimate for the base-2 logarithm of 50 is 44 in $Q3$ or 5.5 in $Q1$.

The DCT remains the same with all the necessary cosine values precomputed-computed, translated into fixed-point and cached.

## 3.2 Testing Conditions

The recognizer used for all of the experiments is part of the JUPITER system. JUPITER provides various weather information such as forecasts, temperatures, wind speeds, and weather advisories for over 300 cities around the world [22]. It is accessible via a toll-free number, and all conversations are recorded for research endeavors. Utterances are transcribed on a regular basis and are added to the training corpus, saving a few for testing purposes. All the utterances then in the training and test

corpora are telephone quality recordings. The test set we used consisted of 1711 utterances deemed clean by the transcriber. The training set consisted of about 120,000 utterances whose MFCCs were computed with a floating-point front-end.

Although the iPAQ was perfectly capable of recording utterances computing fixed-point MFCCs and transmitting them to the server for recognition, not enough data from the iPAQ was available to make a reliable training set. Creating a test set that used iPAQ recorded data also did not make sense because of the mismatch between the 16KHz iPAQ recorded test set and the 8KHz telephone recorded training data. Thus all the experiments done using the fixed-point front-end were performed in a simulated distributed environment, using telephone recorded speech and running it through the fixed-point front-end.

## 3.3 Results

Most of the work from this chapter was done in implementation of the fixed-point front-end. There are, however, several metrics we can look at to examine how this front-end compares to the floating-point front-end. One important metric is looking at the word error rates generated by each. Another way to compare the two front-ends is to look at the computation and storage costs associated with each.

### 3.3.1 Word Error Rate

One expects that because we are discarding information about the speech by doing fixed-point processing, word error rates would increase. However, we found that error rates actually improved. The error rates for the baseline floating-point front-end was 9.8%, and the fixed-point front-end recognizers had a word error rate of 9.6%. To compare the performance, we performed a matched-pair sentence segment significance test. In a matched-pair sentence segment significance test segments of utterances which contain at least two consecutive words both systems recognized correctly. It, then, computes the difference in the number of errors made by each system [15]. The significance test found that the difference between the fixed-point front-end system and the floating-point front-end system was not significant. These recognizers used models trained on clean telephone speech processed by a floating-point front-end. We also retrained our models using the fixed-point features and saw no increase in performance by doing so.

## 3.4 Discussion

Our results show that using the fixed-point front-end improves the performance of the recognizer. We feel this could be because the fixed-point front-end gives an approximation of the coefficients, and is, therefore, not as sensitive to the minor fluctuations in them that could affect recognition. In Chapter 4 we see similar results: as we quantize the coefficients, we can achieve better recognition rates over the baseline.

The system presented here is still far from complete. At this point the system can record data on the iPAQ, quantize it (as discussed in Chapter 4), and send it to the server for recognition, but the recognizer still uses models trained on telephone speech, so there is a fundamental mismatch between the test utterances and the models. Although retraining our models on fixed-point features did not improve recognition, collecting a large corpus, recorded on the iPAQ, is still needed so that an iPAQ recognizer may be built that will achieve comparable recognition rates to the simulations done here. Additionally at this time there is no response sent back to the iPAQ from the recognizer. Having either text or speech response would complete the system.

# Chapter 4

# Quantization of Mel Frequency Cepstral Coefficients

Quantization is a necessary part of any distributed speech recognition system. The bit rate of the system that does not do any front-end computation on the iPAQ is 64Kbps (8 bits $\mu$-law sampled at 8KHz) or 128Kbps (8bits $\mu$-law sampled at 16KHz for wide-band speech). Without quantization of the MFCCs the bit rate of the fixed-point system is 89.6Kbps (14 32-bit integers every 5 ms). In this chapter we will show the methods and results from both scalar and vector quantization of MFCCs.

## 4.1 Quantizer Design

We chose to experiment with non-uniform scalar and vector quantizers. In this section we will discuss how we did bit allocation for both scalar and vector quantizers, effectively choosing the number of levels of the quantizer. We will also discuss how the subvectors were chosen and how the quantizer was actually created.

### 4.1.1 Bit Allocation for Scalar and Vector Quantization

The bit allocation scheme for both our scalar and vector quantizers is basically the same. One could see the scalar quantizer being a special case of the vector quantizer where each subvector consists of just one parameter. The greedy algorithm is described below.

- *Initialize:* For each subvector allocate one bit per coefficient in that subvector.
- *Iterate:* Add one bit to subvector $i$, compute the word error rate for the given bit allocation. Repeat for all subvectors.

- *Assign:* Assign one bit to the subvector that resulted in the lowest error rate. If desired number of bits or error rate is reached, quit. Otherwise return to Iterate step.

There is one case where this algorithm fails. That is when the lowest error rate occurs at more than one bit allocation. In the scalar quantization case we always add the bit to the lowest order coefficient. In the vector quantization case the bit went to the subvector that had the lowest number of bits at present. In addition to limit computational complexity in the scalar case, we capped the number of bits any coefficient could have at 8 bits. In the essence of speed, in the vector case we allocated two bits at a time in the vector case until a total of 30 bits had been reached.

### 4.1.2 Choosing Subvectors for Vector Quantization

Before we can allocate bits to subvectors, we must choose which coefficients go into each subvector. We used two methods of partitioning: a correlation-based method and a knowledge-based method. Correlation-based methods are methods that partition into subvectors based on information contained in the correlation matrix. Knowledge-based partitioning puts consecutive coefficient together. In this way the more important lower-order coefficients are kept together.

We used several methods to come up with an appropriate subvector using the correlation matrix. The first method progressively adds subvectors together based on the average correlation until the desired number of partitions is reached. This process is illustrated in Table 4.1. We start by having 5 subvectors. We find the two most correlated coefficients and put them in a subvector together to yield a partition of 4 subvectors. To compute the correlation between groups that contain more than one coefficient, the average of all the pairwise correlations of all coefficients in each group was computed. As shown in Table 4.1, to find the correlation value between coefficient 1 and the group {4,5}, we averaged the correlations between 1 and 4, 1 and 5 and 4 and 5((.3+.1+.8)/3 = .4). This method was used to develop the subvectors for partition I shown in Table 4.2.

A second method used a set of coefficients as bases for each subvector then clustered the remaining coefficients to the base with which it was most correlated. For example, if we wanted 5 subvectors, we would find the 5 least correlated coefficients by first finding the first pair (just the pair with the lowest correlation coefficient) then adding one coefficient to the set of bases by choosing the parameter that increased the average pairwise correlation in the set the least. Specifically, let each coefficient be represented by $x_i$ and the set of all coefficients be $X$. Let the current base set be $B$ where each base coefficient is represented by $b_j$, the size of $B$ is $n-1$ and $\overline{(A,B)}$ is the average of the pairwise correlations between all elements of $A$ and $B$. Then it

| | 1 | 2 | 3 | 4 | 5 |
|---|---|---|---|---|---|
| 1 | 1 | .6 | .4 | .3 | .1 |
| 2 | | 1 | .4 | .2 | .4 |
| 3 | | | 1 | .1 | .2 |
| 4 | | | | 1 | .8 |
| 5 | | | | | 1 |

| | 1 | 2 | 3 | 4,5 |
|---|---|---|---|---|
| 1 | 1 | .6 | .4 | .4 |
| 2 | | 1 | .4 | .467 |
| 3 | | | 1 | .367 |
| 4,5 | | | | 1 |

| | 1,2 | 3 | 4,5 |
|---|---|---|---|
| 1,2 | 1 | .467 | .4 |
| 3 | | 1 | .367 |
| 4,5 | | | 1 |

Table 4.1: Progression of correlation matrices for the first method of obtaining correlation based subvectors.

| Label | Subvectors | Method |
|---|---|---|
| I | `[0,1,10,11,12,13], [2,3,5,6],[4,8],[7],[9]` | Correlation |
| II | `[0,1,6,7],[2,3,5],[4,8],[9,10],[11,12,13]` | Correlation |
| III | `[0,1],[2,3],[4,5],[6,7],[8,9],[10,11],[12,13]` | Knowledge |
| IV | `[0,1],[2,3],[4,5,6],[7,8,9],[10,11,12,13]` | Knowledge |

Table 4.2: Subvector Partitions for VQ experiments.

can be said that

$$x_i = b_n \quad \text{if } \overline{(x_i, B)} < \overline{(x_j, B)} \quad \forall x_j \in X \setminus B$$

This process of adding parameters to the base set was continued until the size of $B$ reached 5. Now we thought of each base coefficient as the seed for a subvector. We went through each coefficient not included in the base set and assigned them to the subvector with which it had the highest average pairwise correlation.

$$\text{add } x_i \text{ to } b_j \quad \text{if } \overline{(x_i, b_j)} > \overline{(x_i, b_k)} \quad \forall b_k \in B$$

Using this method to come up with a correlation-based partition led to the creation of partition II shown in Table 4.2

In addition to using information obtained from the correlation matrix, we also tried knowledge-based partitioning. In these we simply grouped the coefficients in their numerical order to create subvectors. Two knowledge-based partitions were explored they are given in Table 4.2 partitions III and IV. Partition III simply used pairs of coefficients as subvectors. This partition is different that the others because it uses 7 subvectors. All the other partitions use 5 subvectors. Partition IV was similar to partition III except there are 5 subvectors of varying dimensionality.

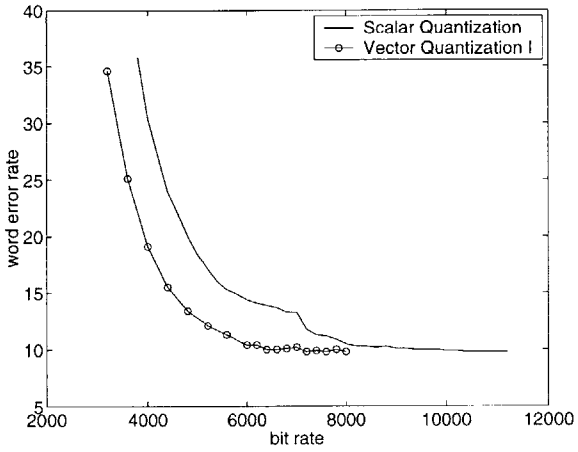


Figure 4.1: Plot of Scalar Quantization versus Vector Quantization.

### 4.1.3 Quantizer Creation

In order to create a non-uniform quantizer, we needed information about the statistics of our MFCCs. We created a random subset of 25000 utterances and computed the MFCCs for each. For scalar quantization then we merely ordered each coefficient and created equal probability bins by putting the same number of seen coefficients in each bin. For vector quantization we use binary splitting with k-means as described in Section 2.4.2.

## 4.2 Results

When comparing quantization schemes, we looked at two aspects: resulting word error rates and computational and storage costs. Here, we compare word error rates from the above bit allocation algorithm for both scalar and vector quantization. In order to choose a reasonable quantizer for the iPAQ, we must also look at the load it puts on the device, so we explore the computational and storage costs for the given quantizers.

### 4.2.1 Word Error Rates

In Figure 4.1 we show the results from the scalar quantization scheme and one vector quantization scheme. The vector quantizer shown here is partition I, but is representative of all of the vector quantizers used. One can see that the vector quantization scheme achieves convergence at a lower bit rate than the scalar quantizer. The bit

| Bit Rate | Bit Allocation | | | | | | | | | | | | | | Word Error Rate |
|---|---|---|---|---|---|---|---|---|---|---|---|---|---|---|---|
| 4000 | 2 | 2 | 2 | 2 | 2 | 2 | 1 | 1 | 1 | 1 | 1 | 1 | 1 | 1 | 30.4% |
| 5000 | 2 | 2 | 3 | 3 | 2 | 2 | 2 | 2 | 2 | 1 | 1 | 1 | 1 | 1 | 18.3% |
| 6000 | 2 | 2 | 3 | 3 | 3 | 3 | 3 | 2 | 2 | 2 | 1 | 2 | 1 | 1 | 14.4% |
| 8000 | 4 | 4 | 4 | 4 | 3 | 4 | 3 | 2 | 2 | 3 | 2 | 2 | 2 | 1 | 10.5% |
| 9600 | 4 | 7 | 4 | 5 | 4 | 4 | 3 | 2 | 3 | 4 | 2 | 2 | 2 | 2 | 10.0% |
| 11200 | 4 | 8 | 5 | 5 | 6 | 5 | 5 | 3 | 3 | 4 | 2 | 2 | 2 | 2 | 9.8% |

Table 4.3: Bit rates, Allocation and corresponding Word Error Rates for Scalar Quantization.

rates, word error rates, and bit allocations for scalar quantization are given in Table 4.3. For this system the baseline floating-point recognizer has a word error rate of 9.8%. The fixed-point recognizer (with no quantization) also has a word error rate of 9.6%. It is interesting to note that with scalar quantization we can reach rates of 9.8%. Again we performed a matched-pair sentence segment significance test [15]. It found that the difference between the fixed-point front-end recognizer and the scalar quantized MFCC recognizer was insignificant. We must also point out that our SUMMIT recognizer has a frame rate of 200 Hz which is uncommon. Most recognizers use a 100Hz frame rate and thus the bit rate would be half what is recorded here.

For the four vector quantization schemes Table 4.4 shows their resulting word error rates at different bit rates. We did not attempt as high bit rates in the vector quantization schemes as in scalar quantization because of the computation and storage costs. However, for the rates explored they all performed equally or better than scalar quantization. We performed a matched pair sentence significance test to compare partition II and partition III [15]. It found that at 8000 bps the recognizers were insignificantly different. Unlike in Digalakis, et al. [4], since the knowledge-based partition was not significantly better than the correlation-based one, we found no appreciable difference between them for product-code vector quantization. Moreover, when we retrained our models using the quantized MFCCs, we saw no improvement.

### 4.2.2 Computational and Storage Costs

To effectively compare the different quantization schemes presented in this chapter, we must also consider the computational and storage costs associated with each. In Section 2.4.2 we give equations to estimate of the computational and storage costs associated with different quantizers. Here, all of our vector quantizers are product code quantizers implemented with binary splitting. Since we perform an indepen-

| Bit Rate | I | II | III | IV |
|---|---|---|---|---|
| 3200 | 34.6% | 22.4% | 38.2% | 35.9% |
| 4000 | 19.1% | 15.2% | 18.3% | 18.1% |
| 4800 | 13.4% | 13.3% | 12.0% | 12.3% |
| 5600 | 11.5% | 12.0% | 10.5% | 10.7% |
| 6400 | 10.0% | 10.8% | 9.8% | 10.1% |
| 7200 | 9.8% | 10.4% | 9.8% | 10.0% |
| 8000 | 9.8% | 9.9% | 9.5% | 9.8% |

Table 4.4: Bit rates, and Word Error Rates for Vector Quantization Schemes.

dent quantization of each subvector and are using a separable distortion measure (mse), we can compute the total computational cost as being the sum of the computational costs of each subvector ($C = \sum_{i=1}^{K} N_i \log_2 L_i$ where $K$ is the total number of subvectors). This figure is reduced by a factor of 2 from the equation quoted in Section 2.4.2 because we are using an mse distortion measure [12]. A plot of the resulting computational costs is shown in Figure 4.2(a).

The storage costs are computed similarly: the storage cost is the sum of the storage costs for each of the subvectors. Since we are using binary splitting, the resulting storage cost is $M = \sum_{i=1}^{K} N_i(L_i - 2)$. Thus, we estimated the storage cost for each of the scalar and vector quantizers proposed in this chapter. Those costs are displayed in Figure 4.2(b). It is important to note that these are merely estimates of the costs. They should be proportional to the actual costs and adequately display the relationships between quantizers.

## 4.3 Discussion

Overall we found that the vector quantizers were more efficient (lower word error rates at lower bit rates) than the scalar quantizer. Although the scalar quantizer had the lowest error rate at 9.8%, we found the difference between the scalar quantizer and the vector quantizer (partition III) that operated at 8000 bps with 9.5% word error rate was not statistically significant. Thus, we concluded that neither quantizer is more accurate than the other. Additionally, we found that the difference in performance between the 4 vector quantizers was not consistent. So, we do not draw the conclusion that the knowledge quantizers outperform the correlation quantizers as was done in [4].

To choose an optimal quantizer for this system, we must think of the trade-off between bit rate and storage and computational costs. Let's consider that we want to

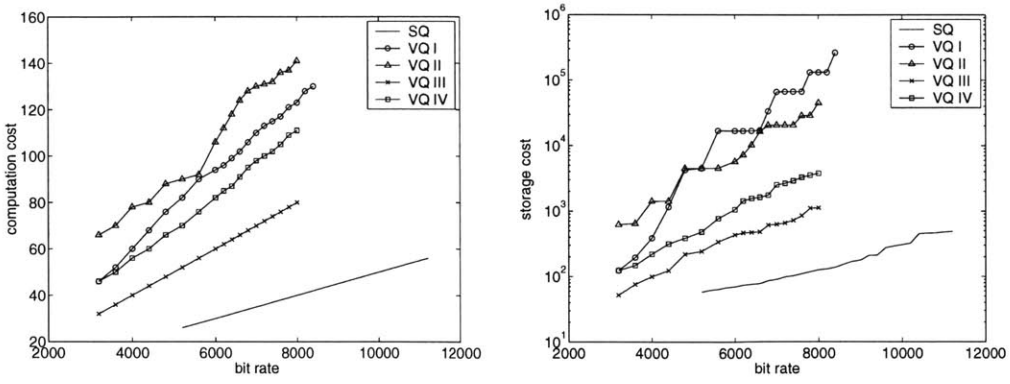


(a) (b)

Figure 4.2: The computation costs for the scalar quantizer and all four vector quantizers are shown in Figure 4.2(a). In Figure 4.2(b) the storage costs for the scalar and vector quantizers are shown.

maintain a word error rate of less than 10%. In experiments we found that we could attain an error rate of 10% at 6400 bps in the vector quantize and 9400 bps in the scalar quantizer. However, at these rates the vector quantizer has a computational cost relative to 66 and a storage cost relative to 484. The scalar quantizer has an approximate computational cost of 42 and a storage cost of 138. Ultimately the decision to use a scalar or vector quantizer should be determined for an individual system preference.

# Chapter 5

# Quantization of Boundary Measurements

Because our segment-based recognizer does not directly use MFCCs as its features, we explored the quantization of the derived boundary measurements. We hoped that if the boundaries were not hypothesized too frequently, we might be able to further reduce the bit rate needed. In addition, because the principle component analysis is incorporated in the computation of the boundary measurements, each coefficient of the features is independent of all others. We hoped to use this fact to our advantage when quantizing. Finally, we wanted to explore the effect on recognition performance because the resulting boundary measurements would be fed directly into the classifier, as opposed to the MFCCs which are further processed, thus, smoothing the quantization error, before being used in the classifier.

Unlike the MFCCs we do not have fixed-point code that computes these boundary measurements. To complete the system that computes boundary measurements on the client, we need to create a boundary detector that works on fixed-point MFCCs using fixed-point operations. Additionally, we need to implement cepstral mean normalization and principle component analysis. The cepstral mean subtraction would be the same as the floating-point version. The principle component analysis can be thought of as a matrix multiplication. That matrix could be computed in floating-point on the server, translated to fixed-point, and cached on the iPAQ. At this point we have not implemented any of these in fixed-point. This chapter focuses on exploring quantization issues that would be faced when fixed-point boundary computations have been implemented.

## 5.1 Quantizer Configuration

Because the length of the boundary measurement feature vector is so long, using our previous bit allocation algorithm was not reasonable for scalar quantizers. For this reason we did several uniform allocations with both scalar and vector quantization. Additionally, we experimented with weighting the bit allocation by the eigenvalues. We also tried using the previous bit allocation method for vector quantization and using a gentle weighting of the lower order coefficients.

### 5.1.1 Uniform Bit Allocation

We varied the number of bits from 2 bits per subvector to 13 bits and the number of coefficients per subvector from 1 to 5. In the 2 coefficients per subvector case, the partitioning began `[0,1]`, `[2,3]`, `[4,5]` and so on. In the 5 coefficient per subvector case, the partitioning looked like this `[0,1,2,3,4]`,`[5,6,7,8,9]` and so on. We then varied the number of bits assigned to a subvector. In each case the same number of bits was used for each subvector; thus, in the 2 coefficient per subvector case if the bit allocation was 2 bits per subvector the total number of bits for the quantizer was 50. In the 5 coefficient per subvector case, if 5 bits per subvectors were used, then the total bit allocation was 50 bits. The results from these quantizers are seen in Section 5.2.

### 5.1.2 Eigenvalue Weighted Bit Allocation

In addition because the principle component analysis removes the linear correlation between the coefficients, exploring correlation-based partitioning did not make sense. For non-uniform bit allocations in the scalar quantizer, we explored using information from the eigenvalues generated for each PCA component when the PCA matrix was computed. We weighted each coefficient relative to its corresponding eigenvalue as given by:

$$w_i \approx N \frac{x_i}{\sum_j x_j}$$

Here, $w_i$ is the weight given to the $i^{th}$ coefficient. N is the total number of bits per boundary, and $x_i$ is the eigenvalue for the $i^{th}$ coefficient. Results for this bit allocation are shown below.

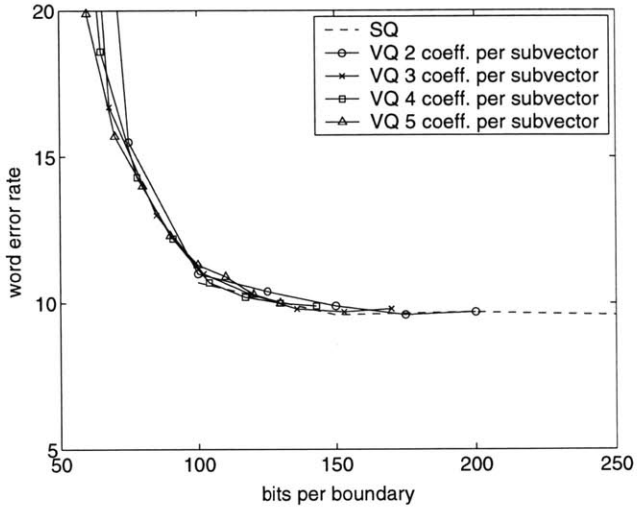


Figure 5.1: Plot of word error rates for various boundary measurement quantization schemes.

## 5.2 Results and Costs

Similar to the experiments that we ran with the MFCCs, we looked at both the word error rates from each quantization scheme and the computational and storage costs for each to determine the empirically optimal quantizer. Those results are reported here.

### 5.2.1 Word Error Rates

We found that overall scalar and vector quantization of the boundary measurements had similar convergence regions as shown in Figure 5.1. All of the quantizers shown here are uniform bit allocation quantizers. From this figure we can see that at very low bit rates vector quantizers with more coefficients per subvector outperformed those with fewer coefficients per subvector. But, as we move to a word error rate range with acceptable performance, all of the quantization schemes are comparable.

With MFCCs we found that we could out perform uniform bit allocation quantization by using non-uniform bit allocation quantization. We thought that the same might be true for boundary measurements. When we compute the principle component analysis rotation matrix, we also compute the eigenvalues for each component. We designed a bit allocation that follows the general trend of the eigenvalues as specified in Section 5.1.2. Using this bit allocation for scalar quantization, we computed the resulting word error rates. Those results are shown in Table 5.1. At 150 bits

| Bits per Boundary | Word Error Rate |
|---|---|
| 107 | 14.3% |
| 150 | 12.1% |

Table 5.1: Scalar quantization results using eigenvalues as guides for bit allocation.

per boundary the uniform scalar quantizer yields a word error rates of 9.6%. The eigen-inspired bit allocations perform over 25% (relatively) worse than the uniform scalar quantizer.

Since using the eigenvalues as a guide did not improve recognition rates, we decided to try a more gradual bit allocation schemes. Because none of these uniform bit allocation quantizers stood out as being better than any of the others, we performed these bit allocations on a vector quantizer with 5 coefficients per subvector. We explored using the bit allocation algorithm (adding 2 bits at a time) to go from 50 bits to 60 bits. These results are shown in Table 5.2. In the first and second rows we report the error rates for uniform bit allocations of 50 and 60 bits. In the third row the results from the bit allocation algorithm are shown. Although the difference between the uniform 60 bit allocation and the non-uniform 60 bit allocation were found significant at a level of 0.009 by a matched-pair sentence segment significance test [15], we decided not to further pursue using the bit allocation algorithm. Additionally, we tried just a simple knowledge-based allocation as seen in the last row of Table 5.2. Here we just set the first 5 subvectors to have one more bit and the last 5 subvectors to have one less bit, thus not changing the total number of bits per subvector, but putting more resolution on the lower order coefficients. We found this strategy also did not give us any improvement over uniform bit allocation.

### 5.2.2 Computational and Storage Costs

The underlying computational and storage costs for vector quantizers are discussed in Section 2.4.2. In Figure 5.2 we have plotted the theoretical computational and storage costs for the uniform bit allocation scalar quantizer and 4 of the uniform bit allocation vector quantizers. The general trend shown in the graph is that for every additional bit added per subvector the storage cost doubles, and the computational cost increases linearly. Since the word error rate seems to be independent of the quantizer for low word error rates, we should choose the quantizer with the lowest computational and storage costs. Here, it is clear that the best choice is the scalar quantizer.

| Bits per Boundary | Bit Allocation | | | | | | | | | | Word Error Rate |
|---|---|---|---|---|---|---|---|---|---|---|---|
| 50 | 5 | 5 | 5 | 5 | 5 | 5 | 5 | 5 | 5 | 5 | 32.3% |
| 60 | 6 | 6 | 6 | 6 | 6 | 6 | 6 | 6 | 6 | 6 | 19.9% |
| 60 | 7 | 5 | 7 | 9 | 5 | 7 | 5 | 5 | 5 | 5 | 18.9% |
| 100 | 10 | 10 | 10 | 10 | 10 | 10 | 10 | 10 | 10 | 10 | 11.3% |
| 100 | 11 | 11 | 11 | 11 | 11 | 9 | 9 | 9 | 9 | 9 | 11.3% |

Table 5.2: All of the results shown in this table are for a vector quantizer with 5 coefficient per subvector. The first two rows of this table show bit allocation and word error rates for uniform distribution of 50 and 60 bits per boundary. The third row shows bit allocation and word error rates for the 60 bits per boundary (non-uniform bit allocation vector quantizer). The next to the last row shows the uniform bit allocation for a total of 100 bits per boundary, and the last row shows the word error rate and bit allocation for a gently weighted non-uniform bit allocation.

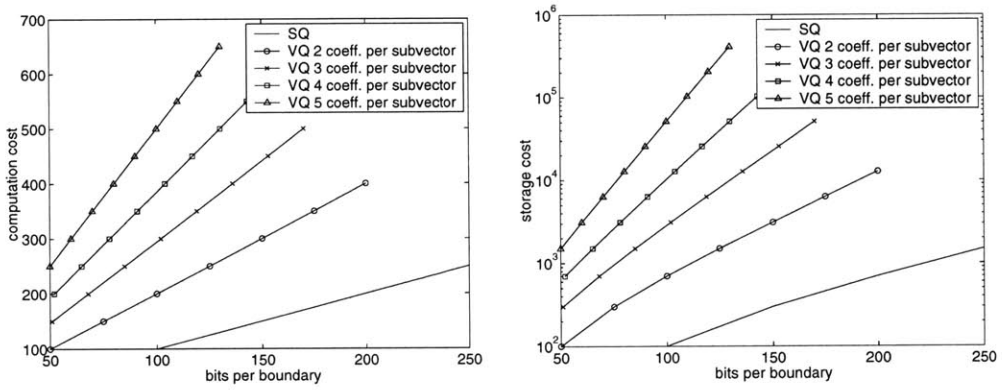


(a) (b)

Figure 5.2: The computation costs for the scalar quantizer and all four vector quantizers are shown in Figure 5.2(a). In Figure 5.2(b) the storage costs for the scalar and vector quantizers are shown.

| Type | Bit Rate | Word Error Rate |
|---|---|---|
| Boundary, SQ, 3 bits per coefficient | 3315 | 9.6% |
| Boundary, SQ, 4 bits per coefficient | 4420 | 9.7% |
| Boundary, SQ, 5 bits per coefficient | 5525 | 9.6% |
| MFCC II | 3200 | 22.4% |
| MFCC III | 4800 | 12.0% |
| MFCC III | 5600 | 10.5% |

Table 5.3: Bit rates and word error rates for quantizing boundary measurements versus MFCCs.

## 5.3 Discussion

In comparing the performance of the scalar quantizers with the vector quantizers (using uniform bit allocations), we saw no significant difference. At the very low bit rates the vector quantizers with more coefficients per subvector outperformed those with less. However, at those very low bit rates the word error rates were so unattractive they would not rationalize the very low bit rate. It is not surprising that these quantizers performed similarly. Vector quantizers exploit the statistical dependence between coefficients to yield better results over the scalar quantizers. In quantizing the boundary measurements, we are quantizing coefficients that have been decorrelated. Since each coefficient is approximately independent of all other coefficient using vector quantization can give little improvement over scalar quantization schemes.

Our results showed that changing the bit allocation from a uniform to a non-uniform scheme had little effect on the word error rate. We know that the lower order coefficients have higher variances than the higher order coefficients and are thought to be the more important of the coefficients. Therefore, that no non-uniform bit allocation outperformed the uniform bit allocation is surprising. This result may be explained by the fact that we do not know how the classifier weights these coefficients. With MFCCs we know that the lower order coefficients give the general spectral shape, but here, after the principle component analysis, it is not clear which of these coefficients are most important to the classifier. From these experiments the empirically optimal quantizer is the uniform bit allocation scalar quantizer. In addition we performed a matched pair sentence significance test [15] and found the difference between the baseline and the scalar quantizer to be insignificant. Thus, we have not degraded performance by quantizing our boundary measurements.

Because boundaries are not proposed at uniform intervals, the bit rate is hard to estimate. On our test set we averaged 21.1 boundaries per second. At this rate the bit rates and word error rates for the uniform scalar quantizer of boundary measurements

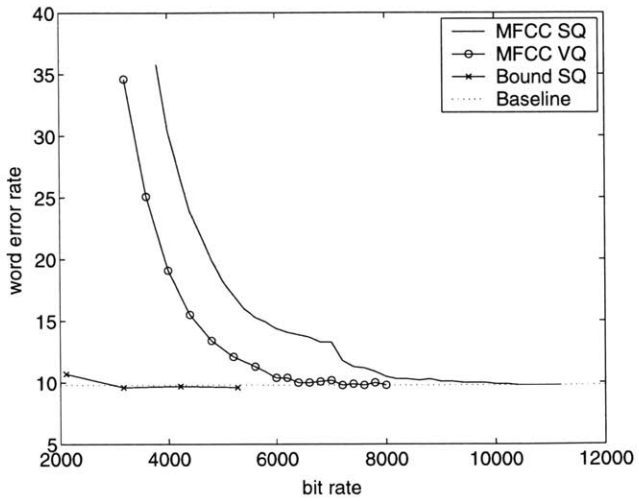

Figure 5.3: Overall performance of quantized recognizers.

and those for several MFCC quantizers are shown in Table 5.3. A plot of the overall performance is given in Figure 5.3.

In this table the boundary measurement quantizers are all uniform scalar quantizers with the number of bits per coefficient indicated in the Type column. The results from vector quantizers of the MFCCs that are of similar rates to those from the boundary measurement quantizers are reported here. Which MFCC quantizer was used in indicated by the roman numeral in the Type column and corresponds to the label definitions in Table 4.2. Despite having the unquantized values of the boundary measurements going straight into the classifier, the boundary measurement quantizer outperforms the MFCC quantizer on this range. Also if we were to look at the number of hypothesized boundaries per second as a function of word error rate, for the word error rate of 10.5% the MFCC quantizer achieves a bit rate of 5600 bps. For the boundary measurement quantizer to maintain a lower bit rate, boundaries can be hypothesize at most 44 times per second.

Clearly, since quantizing the boundary measurements does not degrade performance, and since they are hypothesized so infrequently, a DSR system using a segment-based recognizer should implement the computation of boundary measurements on the client.

# Chapter 6

# Conclusions

In this thesis we aspired to improve upon our existing iPAQ DSR system. By moving the transmission point to after the signal processing, we hoped to both reduce the bandwidth required and not degrade performance. What follows is a summary of the work completed in this thesis and proposed future directions for this work.

## 6.1 Summary

By creating a fixed-point front-end, we endeavored to reduce the computations necessary to compute the features on the iPAQ. This was supported by work by Hewlett Packard [3]. We carried out all of our experiments in a simulated DSR environment using telephone speech recorded from our JUPITER system and processing with the fixed-point front-end. We found that although there is some loss of resolution by using fixed-point numbers and special fixed-point approximations of the magnitude and the natural log, using our fixed-point front-end did not degrade the performance of the recognizer. However, using the fixed-point MFCCs actually increased our bit rate from 64Kbps for the original system to 89.6Kbps in the fixed-point system.

To combat our increase in bit rate due to using the fixed-point front-end, we explored different quantizers for MFCCs. We evaluated both scalar and vector quantizers using a bit allocation algorithm given in [4, 12]. Neither quantizer outperformed the other in terms of accuracy. However, the vector quantizer was more efficient: reaching error rates at lower bit rates than the scalar quantizer. Still, the scalar quantizer was far less computational intensive and used far less memory.

Finally, because our recognizer further processes MFCCs to arrive at boundary measurements, we explored the idea of quantizing boundary measurements. We found that quantizing the boundary measurements outperformed quantizing MFCCs. Due to the independent natures of the features within the boundary measurements we

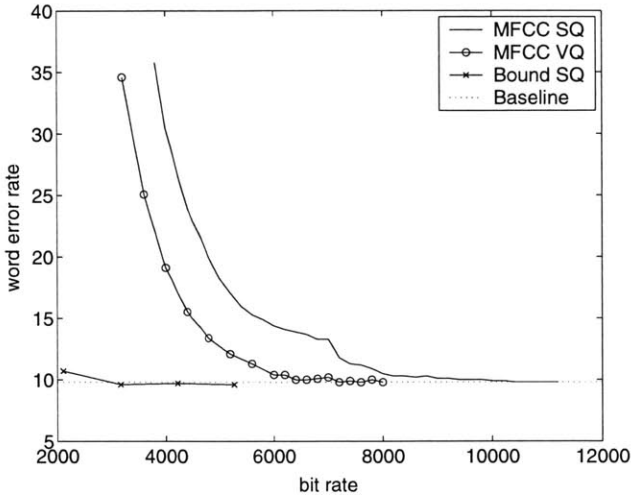

Figure 6.1: Overall performance of systems.

could implement a uniform bit allocation scalar quantization scheme that performed similarly to the vector quantizer yet had lower computational and storage costs. Moreover, the boundary measurements were proposed on an average of 21.1 times per second, thus even lower bit rates could be arrived at by quantizing the boundary measurements. A plot of the overall performance of the systems described here is shown in Figure 5.3 and reproduced here.

## 6.2 Future Directions

As described in Chapter 3, there remains much work to do to have a complete DSR system. Collection of a large database of iPAQ recorded data is a start. Creating a fixed-point computation of boundary measurements and quantizers is also necessary for creating a complete system.

To have a system that takes advantage of the low error rates and bit rates achieved by the boundary measurement quantizer, the boundary measurements must be computed on the iPAQ. The biggest task in this implementation is designing for a fixed-point boundary detector. With this complete, cepstral mean subtraction and computing the full boundary measurements would be simple. Additionally, the principle component analysis matrix could be computed on the server and cached in fixed-point on the iPAQ itself.

Although the quantizers parameters could be computed ahead of time in floating-point, the quantizers themselves would need to be translated into fixed-point and stored on the iPAQ. Currently all the quantizers except the scalar MFCC quantizer

expect floating-point numbers and operate in floating-point themselves. However, we do already have a bit packer implemented which sends packets of features to the server.

Ideally, this system would eventually fold into the iPAQ itself. With natural language processing done on the server side after recognition and a resulting command sent back to the iPAQ for execution. Additionally, a conversational system could be built with speech synthesis being performed on the iPAQ itself. The iPAQ could store phones and the information for how to concatenate these phones could be sent from the server [21].

This thesis shows great promise for the implementation of a DSR system with both a fixed-point front-end and fixed-point boundary detector for the iPAQ. This system would both decrease bit rate and leave accuracy unaffected. However, the trade-off between low bit rates and the storage costs associated with the boundary measurement quantizer would have to be weighed to design an optimal DSR system for the iPAQ.

# Bibliography


[1] J. W. Crenshaw. 2000. *Math toolkit for real-time programming.* Lawrence, Kansas: CMP Books.

[2] S. B. Davies and P. Mermelstein. Comparison of parametric representations for monosyllabic word recognition in continuously spoken sentences. *IEEE Trans. Acoustics, Speech and Signal Processing*, vol. ASSP-28, no. 4, pp, 357-366, Aug. 1980.

[3] B. W. Delaney, M. Han, T. Simunic, and A. Acquaviva. "A low-power, fixed-point, front-end feature extraction for a distributed speech recognition system," *HP Laboratories Technical Report,* HPL-2001-252, Oct. 9, 2001.

[4] V. Digalakis, L. Neumeyer, and M. Perakakis. Quantization of Cepstral Parameters for Speech Recognition over the World Wide Web. *IEEE Journal on Selected Areas in Communications*, Vol. 17, No. 1, pp. 82 - 90, Jan. 1999.

[5] ETSI ES 201 208 V1.1.2: "Speech processing, transmission and quality aspects (STQ); Distributed speech recognition; Front-end feature extraction algorithm; Compression algorithms," Available at www.etsi.org, Reference RES/STQ-00018, Apr. 2000.

[6] M. E. Frerking. 1994. *Digital signal processing in communications systems.* New York: Van Nostrand Reinhold.

[7] S. Furui. Cepstral analysis technique for automatic speaker verification. *IEEE Trans. Acoustics, Speech, and Signal Processing*, vol. 29, no. 2, pp. 254 - 272, Apr. 1981.

[8] J. R. Glass. A probabilistic framework for segment-based speech recognition. *Computer Speech and Language*, vol. 17, issues 2 - 3, pp. 137 - 152, Apr. - July 2003.

[9] W. Gunawan and M. Hasegawa-Johnson. PLP coefficients can be quantized at 400 bps. In *Proc. European Conf. on Speech Communication and Technology*, pp. 77 - 80, Salt Lake City, 2001.

[10] H. Hermansky and N. Morgan. RASTA processing of speech. *IEEE Trans. Speech and Audio Processing*, vol. 2, no. 4, pp. 578 - 589, Oct. 1994.

[11] H. K. Kim and R. V. Cox. A bitstream-based front-end for wireless speech recognition on IS-136 Communications System. *IEEE Transactions on Speech and Audio Processing*, vol. 9, no. 5, pp. 558 - 568, July 2001.

[12] J. Makhoul, S. Roucos, and H. Gish. Vector quantization in speech coding. *Proc. IEEE Special Issue on Man-Machine Voice Communication*, vol. 73, no. 3, pp. 1551 - 1588, Nov. 1985.

[13] A. V. Oppenheim and R. W. Schafer. Homomorphic analysis of speech. *IEEE Trans. Audio and Eletroacoustics*, vol. AU-16, pp. 221-228, June 1968.

[14] A. V. Oppenheim and R. W. Schafer. 1989. *Discrete-time signal processing.* Englewood Cliffs, NJ: Prentice Hall.

[15] D. S. Pallett, W. M. Fisher, and J. G. Fiscus. Tools for the analysis of benchmark speech recognition tests. In *Proceedings International Conference on Acoustics, Speech, and Signal Processing.* pp 97 - 100. Albuquerque, NM. April 1990.

[16] W. H. Press, B. P. Flannery, S. A. Teukolsky, and W. T. Vetterling. 1993. *Numerical Recipes in C, 2nd Ed.* Cambridge: Cambridge University Press.

[17] T. F. Quatieri. 2002. *Discrete-time speech signal processing: principles and practice.* Upper Saddle River, NJ: Prentice Hall PTR.

[18] L. Rabiner and B. H. Juang. 1993. *Fundamentals of speech recognition.* Englewood Cliffs, NJ: PTR Prentice-Hall, Inc.

[19] L. R. Rabiner and R. W. Schafer. 1978. *Digital processing of speech signals.* Englewood Cliffs, NJ: Prentice-Hall, Inc.

[20] B. Sklar. 1988. *Digital communications.* Englewood Cliffs, NJ: PTR Prentice Hall.

[21] J. Yi. "Corpus-Based Unit Selection for Natural-Sounding Speech Synthesis." *Ph.D. Thesis.* MIT. June, 2003.

[22] V. Zue, S. Seneff, J. R. Glass, J. Polifroni, C. Pao, T. J. Hazen, and I. L. Hetherington. JUPITER:A Telephone-based conversational interface for weather information. *IEEE Transactions on Speech and Audio Processing*, vol. 8, no. 1, pp. 85 - 96, January 2000.